Energy Storage and Conversion 2026, 4(1), 4099.
doi: https://doi.org/10.59400/esc4099

Article

Solar box recovery of mixed-wax candle fragments and reuse on the island of Crete

Victor John Law[1,*], James F. Lalor[2], Jenny Magnes[3], Denis Pius Dowling[1]

[1] School of Mechanical and Materials Engineering, University College Dublin, D04 V1W8 Dublin, Ireland
[2] School of Mechanical Engineering, Technological University Dublin, D01 K822 Dublin, Ireland
[3] Physics and Astronomy Department, Vassar College, New York, NY 12604, USA
*** Corresponding author:** Victor John Law, viclaw66@gmail.com

CITATION

Law VJ, Lalor JF, Magnes J, et al. Solar box recovery of mixed-wax candle fragments and reuse on the island of Crete. Energy Storage and Conversion. 2026; 4(1): 4099. https://doi.org/10.59400/esc4099

ARTICLE INFO

Received: 27 January 2026
Revised: 6 March 2026
Accepted: 11 March 2026
Available online: 18 March 2026

Abstract: This paper investigates the proof of principle of small-scale off-grid solar thermal batch recovery of candle wax on the island of Crete in astronomical winter season, where the Sun's irradiance is in the range of 820–940 W·m^{-2}. The investigation was carried out based on the recovery of unconsumed mixed petroleum-based paraffin and plant-based soy and palm-wax (250 g each) candle fragments and their re-casting into new 50–60 g blended-wax candles. Based on a converted family size (27 L) solar box cooker the investigation is conducted during the spring equinox of March 2025 and the winter solstice in December 2025. The solar box cooker conversion extends its functionality from simple food cooking and culinary leaf dehydration to the circular economy of mixed-wax fragments recovery and reuse thereby increasing the cost-benefits of the cooker. Sensible heat measurements and latent heat of fusion calculations for the solar wax recovery process are explored; in terms of solar box cooker energy conversion to applied power (W, or J.s^{-1}) into the wax phase-change process, wax energy budget (J), and wax energy density (J.g^{-1}). The challenge in sourcing pre-used temporary and permanent molds is explored along with solar heated water used for releasing of the blended wax From a circular economy perspective, the off-grid solar box cooker design allows future scaling-out to a possible 1 kg of mixed-wax recovery, when solar processing is performed at, or around, the time of the summer solstice where solar irradiance is strongest (typically, 1,020 W·m^{-2}) and increased available daylight hours allow a third, and possibly a fourth 250 g of mixed-wax to be recovered and re-cast.

Keywords: solar box cooker; candle wax; wax recovery; wax re-casting; thermodynamics

1. Introduction

The use of a solar box cooker (SBC) for leaf dehydration variant is an example of a sustainable green, technology, as the dehydration process does not use: electricity, gas, oil, or biomass as the source of enabling energy [1–4]. Amongst the considerations for selecting the use of SBC is economics, for example, as to how much money is saved when using solar energy in comparison to an equivalent non-solar energy source. The environmental impact is also a consideration, for example, the notional amount of CO_2 emissions being prevented from going into the environment. These are two important factors influencing the world-wide up-take of solar cookers and their variants [5,6]. Recently, prototype photovoltaic panels assisted solar wax melters [7,8]

and commercial linear fresnel reflector assisted solar wax melter has been reported [9], where the investment is paid back by the sale of the candles. Such investment for small-scale family solar melter however can be prohibitive.

To enhance the thermal performance of the SBC, non-food contaminating phase change materials (PCM) in particular wax have been investigated [5, 10, 11], plus how to cook food in unfavorable weather conditions [12], and in mountainous regions where daylight hours are limited [1, 2, 4, 13]. Indeed, on the island of Crete, where violent winter storm systems occur that bring down overhead power lines and disrupt road transport links and cut off remote communities [14], it has been proposed that a winterized SBC [2] can be included in a family emergency/disaster preparedness plan. A perceived drawback of these SBC/SBC-d devices is local overheating which can lead to undesirable food product quality [15, 16]. On the island of Crete, a further consideration when using SBC/SBC-d is that it is susceptible to windblown Sahara dust [17] and microorganism and bacteria species episodes at and around the spring equinox [18]. Nonetheless, when it comes to solar-recovery of unconsumed wax fragments for the production of new candles such drawbacks become less important. Indeed, the incorporation of sand-wax formulations used for candles makes for a marketable textured candle [19].

On the island of Crete, as on many other Greek islands, the growing amount of waste in the take-make-use-dispose linear economy has been acknowledged, if not acted upon [20]. Adopting the reuse-repurpose-recycle circular economy is one goal of green chemistry [21,22]; thus applying this practice to the recovery of unconsumed candle wax fragments and reuse as household emergency lighting, religious festivals, mood lighting, and mosquito repellents is an example of green chemistry being put into practice. To be of practical use solar mixed-wax recovery needs to be performed all-year-round. For example, the months covering Christmas and Easter celebrations and in the astronomical summer season when there is an influx of tourists to the island. Running parallel to these two seasons there is a socio-economic value in the giving and receiving of handcrafted gifts, and the bartering for fair prices of services and goods, both of which are hallmarks of sustainable green values [23]. Waste recovery however can be energy-intensive and complex in waste repurposing [24] and is of particular concern in the Cretan astronomical winter season (December through March) where the Sun's irradiance is of the order of 800–920 $W \cdot m^{-2}$ on sunshine days that are between 9–10 h [2]. In addition, the collection and repurposing of suitable containers for candle molds can be a challenge for the small-scale candle-maker. Therefore the aim of this work is fourfold.

1) The repurpose of a portable off-grid family size (27 L) SBC [1,2,4] for the solar recovery of mixed-wax candle fragments on the Mediterranean island of Crete at a mountain village location (35.31° N, 24.31° E, altitude 150 m). The solar wax recovery and re-casting is performed during the months of December through March where sunshine daytime temperatures range between 10–18 °C making wax recovery a challenge. The days in question are: 1st and 15th March 2025 (spring equinox 21st March, providing nearly equal daylight and darkness hours) and a target day close to the 21st–22nd December 2025 (winter solstice, shortest

day, least direct sunlight in the northern hemisphere), weather permitting.

2) Estimate the SBC required power, process energy budget, and energy density for the recovery of mixed-wax fragments, using both sensible heat and phase-change calculations.

3) Extend the SBC functionality (without incurring non-renewable energy costs) by re-casting the recovered mixed wax into suitable molds (glass, metal, or plastic containers) for the production of 50–60 g pillar candles. Where free-standing pillar candles are required, use solar-heated water (70 °C) to thermally release the wax candle from its mold.

4) With aims 1, 2, and 3 achieved, make a meaningful comparison of the calculated solar power, energy, and energy density of solar mixed-wax recovery process with solar-cooked food (whole liquid eggs, white medium-grain rice and brown Lentils rice and lentils) within a similar design and volume SBC [1, 2, 4] at the same geographical coordinates, and astronomical seasons.

2. SBC-m design

The SBC-m, where m, stands for melt, is a step-wise development from the SBC-s [1] and SBC-w [2] through to a solar dehydrator SBC-d [4] (where s, w, and d denote mode of operation: summer, winter, and dehydration. The SBC-m is constructed from locally sourced sustainable plywood sheets to produce a 27 L cuboid-like structure (width = 32 cm, depth = 36 cm, rear height = 29 cm and front height = 20 cm, all internally lined with Aluminum foil) topped with a 2 cm thick double-glazed window (aperture area = 0.1 m^2) set at 31 degrees and fitted tight to the SBC frame to stop air-flow through the structure, thereby the SBC-m operates in the closed-greenhouse mode. The SBC-m employs one external reflector panel angled to produce a SBC virtual incident collection area (A_i) = 0.196 m^2, where A_i is defined by the diagonal distance between the external reflector panel top edge and the front edge of the SBC-m multiplied by the SBC-m width. For winter use, a 15° truncated wedge is used to tilt the SBC window towards the Sun's altitude in the winter sky. The SBC-m weighs approximately 18.2 kg including a 2.5 kg tripod mount for easy orientation to the Sun's azimuth position **Figure 1.** Specific SBC-m design features include:

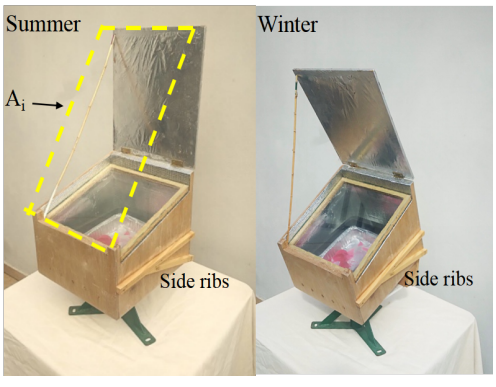

(a) **(b)**

Figure 1. **(a)** Photograph of the SBC-m set for summer operation with its virtual incident collection area (A_i) outlined with yellow dashed lines; **(b)** Photograph of SBC-m set for winter operation.

A new and dedicated heat absorber plate is used to prevent contamination with SBC modes of operation. The dimension of the absorber plate is 0.08 cm thick dark enameled steel sheet cooking vessel with rolled edge (length = 28.5, width = 23, and depth = 6 cm. Two wooden side-ribs (cross-section 1.5 × 15 cm) are used to support candle wick holders). The first set is positioned for summer use with the centerline 9.5 cm from the SBC-m base. The second set is for winter use and is set at 15°.

Build cost and cost comparison

The build cost of the SBC-m was 162 Euro (May 2025), based on materials and labor, which were sourced locally. A comparison of these costs with other SBCs built after 2022 can be found by Misra et al. [6] and Al-Rajhi et al. [7]. For example, Benbaha et al. [25] provide a 2023 guide price of €223 to €335, Kumar et al. [5] provide a cost of €45 to €143; and Kumar et al. [26] provide a price guide of approximately 48 US dollars.

3. Candle wax

The ancient Egyptians are often cited among the first civilizations to use rushlights, or torches, by soaking the pithy core of reeds in melted animal fat. The absence of soot on the ceilings of painted pharaonic tombs however suggests direct sunlight, (such as at Abu Simbel) and reflected sunlight via mirrors into their temples and tombs. With efficient ventilation, the use of oil wick lamps, that burnt with animal (tallow) or plant-based oils was to illuminate the inner tombs' recesses without the accumulation of soot, is also acknowledged. Wicked candles made by dripping tallow over rolled papyrus are more associated with the beginning of the Ptolemaic Roman Empire. By the time of the Middle Ages beeswax candles with their clean and sweet-smelling burning properties became established throughout the Mediterranean. But due to the prohibitive expense of production, they were generally limited to church ceremonies and used by wealthy individuals. The growth of the whaling industry in the late 18th century brought major changes to candle making, when spermaceti (a wax obtained by crystallizing sperm whale oil) became available in quantity. Like beeswax, the spermaceti wax produces a significantly brighter flame with reduced acrid smoke emissions when burned. Being harder than either tallow or beeswax, Spermaceti wax is more resistant to softening or bending in the summer heat. By the early to mid 1800s, large-scale production of paraffin wax replaced tallow and spermaceti to reduce the acrid smoke and smells home. Stearic acid which has a structural formula of $CH_3(CH_2)_{16}COOH$ is derived from tallow and was found to harden the wax, increase its opacity, and increase the blended wax melting point. At the other end of the hardness spectrum, however liquid olive oil (typical < 50% by weight of the candle) produces a soft and cost-effective solid olive oil candle wax which needs to be used in a candle container.

From today's environmental awareness perspective, wax production poses several environmental and ethical challenges. For instance, free-standing pillar candles and tealights [27–29] contain specific non-renewable petroleum-based paraffin formulations. Whereas plant-based palm and soy wax are biodegradable and renewable but have complex ethical problems arising from deforestation, biodiversity

loss and human rights issues, which are sometimes mitigated by local employment and with manageable sustainable goals [30]. With global bee populations falling (due to habitat degradation and industrial scale exploitation [31]) the relatively high cost of the wax helps to highlight sustainable and ethical (vegan) concerns.

3.1. Petroleum-based paraffin

Paraffin wax is made up from high molecular weight linear *n*-Alkanes with a molecular formula C_nH_{2n+2}, where n represents the number of atoms in the carbon chain (typically = 22 to 27) with a melting temperature range of 49 to 66 °C [5,9,26–29,32–34]. Complete stoichiometric combustion of paraffin wax (where the *n*-Alkanes carbons chain = 25 and 32 oxygen (O_2) molecules can be written as Equation (1), where the products are carbon dioxide (CO_2, g) and water vapor (H_2O, (*l*) [35]) along with the approximate amount of energy released.

$$C_{25}H_{52}(s) + 38O_2(g) \rightarrow 25CO_2(g) + \ 26\ H_2O\ (l) : \Delta H \sim -15,800\ \text{kJ.mol}^{-1} \quad (1)$$

This reaction is driven by the large negative enthalpy (ΔH) and large positive entropy change (ΔS), resulting in a large negative Gibbs free energy (ΔG) of the order of $-14{,}500$ kJ.mol^{-1}. Once the activation energy is reached the reaction is spontaneous and continuous, generating both heat and light (*vh*) until all the wax is burnt. This chemical reaction is informative for well trimmed wicks and no air drafts conditions, but under stress conditions (start of burn-long wicks, air drafts and poor ventilation) that causes incomplete combustion, resulting in soot production in the form of elemental carbon and equivalent black carbon fine particles ($PM_{2.5}$) plus volatile CH and CHO and NO fragments [27,28], where the cracking process proceeds by C-C bond β-scission (~408 kJ.mol^{-1}) rather than C-H bond cleavage (~418 kJ.mol^{-1}) [36].

3.2. Bioparaffins

Biodegradable soy wax, palmitic wax, and beeswax are sometimes termed 'bioparaffins' as they are alternatives to paraffin. From a chemical viewpoint these wax compounds vary in the molecular structure. For example:

Soy wax is derived from cleaned and cracked soybeans, followed by a hydrogenation process to chemically transform the unsaturated fats into *n*-Alkane saturated fatty acids (typically $n = 16$ carbon atoms), and once cooled the product forms a cream off-white wax flak or pellet. Depending on the process the wax has a melting range of 49–82 °C, the lower melting point wax being used in tealights, and where the blending of stearic acid increases the wax melting point making the wax suitable for free-standing pillar candles [33, 37]. Equation (2) presents the stoichiometric combustion formula of stearic acid, along with the approximate energy released.

$$C_{18}H_{36}O_2(s) + 26(g) \rightarrow 18CO_2(g) + \ 18\ H_2O\ (l) : \Delta H \sim -11,290\ \text{kJ.mol}^{-1} \quad (2)$$

Under these non-stress conditions, soy wax has a long clean burn quality compared to paraffin. However, when soy wax is melted below flame temperature and interacts with non-wax elements (color dyes and other debris), its translucent color turns dark

ivory; due to alterations in the soy microcrystal structure [38]. This transformation is of particular interest to candle makers seeking a different color in their candles.

Palm wax is derived from palm oil that has undergone a hydrogenation process to transform its unsaturated fats into linear chain-carbon saturated *n*-Alkanes, the most predominant being palmitic acid that has a structural formula of $CH_3(CH_2)_{14}COOH$. The resultant wax has a hard crystalline texture with a melting temperature range of 50–65 ℃ with a slow and clean burn quality compared to paraffin [33, 39]. Equation (3) gives the complete stoichiometric combustion formula, along with the approximate energy released.

$$C_{16}H_{32}O_2(s) + 32O_2(g) \rightarrow 16CO_2(g) + \ 16\ H_2O\ (l) : \Delta H \sim -9,900\ \text{kJ.mol}^{-1} \tag{3}$$

Botanical essential oils added to soy and palm wax melts (typically, 2–8% by weight of the candle and added at low melt temperature to prevent loss of the volatile fragrance) are considered to offer therapeutic sleep benefits [40]. Whereas fragrance oils when added to the wax melt, are designed to give a consistent strong aroma (good throw) when heated.

Comparing the limited homologous combustion reaction series (1, 2, and 3), it is shown that ΔH falls as the *n*-Alkane carbon-chain is reduced along with the amount of oxygen required for complete combustion (38 to 32 to 26 O_2 molecules). Thus for a burning wax-wick-flame reaction zone surrounded by air (approximately 21% O_2 and 79% N_2), mass transport of fresh O_2 into, and CO_2 out, of the reaction zone can impact burn quality of the paraffin and to a lesser extent palm wax and soy wax. That is, the supply of O_2 becomes the reaction rate-limiting factor where the onset is reached first in the case of paraffin wax followed by palm and soy wax.

3.3. Insect-based paraffin

Insect-based beeswax differs from plant-based wax as it is sourced from honeycomb that bees build in their hives where they store their winter food, and form cells for their eggs and pupae. The wax has a narrow melting point range of 62–64 ℃: attributed to its complex molecular make-up that is dependent on factors such as bee subspecies, diet, and geographical location. The wax consists of *n*-Alkane fatty acid, fatty alcohols, and a complex mixture of esters. The primary mono-esters (35–45%) have a general formula $C_nH_{2n+1}COOC_mH_{2m+1}$, derived from palmitic acid. Followed by die-esters (8–12%) and to a lesser extent tri-esters and higher order esters, along with varying local floral content gives the wax its unique characteristics [7–9, 41]. Beeswax candles burn longer and cleaner than paraffin candles of the same size and weight. The blending of petroleum-based paraffin wax with beeswax decreases candle cost and enables candles to be marketed as a bioparaffin product. Blending beeswax with soy wax produces a semi-solid oleogel which is an important process in reducing unsaturated fats in the food industry with the aim of manufacturing healthier food products [38]. Beeswax has a time and place variable formulation; therefore, its complete combustion formula is difficult to reconcile with its position within the limited *n*-Alkane homologous combustion reactions (1, 2, and 3). For this reason

no further small-scale mixed-wax solar recovery developed in this work. But for comparative purposes beeswax thermal properties are given in **Table 1**.

Table 1. Thermal properties of paraffin, palm, soy wax and beeswax.

Wax-material	Melting point (℃)	Specific heat capacity ($J.g^{-1}.℃^{-1}$)	Latent heat of fusion ($J.g^{-1}$)	Reference
Paraffin wax	49–66	2.5 ± 4	185 ± 35	Kumar et al. [5], Al-Rajhi et al. [7], Al-Rajhi et al. [8], Khan et al. [9], Kumar et al. [26], Andersen et al. [27], Eremkin and Ponomareva [28], Wattanakasiwich et al. [29], Zmywaczyk et al. [32], Eštoková and Kapalo [33], Rezaei et al. [34], Birk and Lawson [35]
Soy wax	49–82	-	119.5 ± 2.5	Eštoková and Kapalo [33], Trisnadewi et al. [37], Sena et al. [38]
Palm wax	50–65	4 ± 2	164 ± 28.5	Eštoková and Kapalo [33], Alakali et al. [39]
Estimated range for equal parts of Paraffin, palm and soy	49.3–75	3.2 ± 1.6	156.3 ± 22	
Beeswax	62–64	1.2 ± 1.3	177.5 ± 32.5	Al-Rajhi et al. [7], Al-Rajhi et al. [8], Khan et al. [9], Putra et al. [41]

Note: Row 5 lists the average thermal properties of paraffin, palm, and soy wax.

Table 1 reports the generally accepted thermal properties for the four candle wax compounds. Given these limited data, the specific heat capacity and latent heat of fusion values mirror the variation in their melting temperatures. Consequently, recovering unconsumed candle wax fragments of different types means that as wax types are melted to form a new physical blend, their solid-liquid phase transition temperature will vary from one wax batch to another. For example, **Table 1**, row 4, gives an estimated range for equal parts of paraffin, palm and soy wax.

3.4. Mixed-wax waste

There are several geometrical, environmental, and improper first-time burn factors that lead to non-uniform candle burning and the non-combustion of wax, and ultimately the generation of waste wax. **Figure 2a–c** provides examples of these problems according to their propensity to form waste.

a) Wax stub waste: where the candle base at the candle holder (whether metal or glass) becomes difficult or unsafe to burn **Figure 2a**.
b) Tunneling occurs when the first burn does not produce an even melted wax pool between the flame and the candle rim, flame that induces a burn memory ring. Without this memory ring, the inner-core burns straight down whilst wasting the relatively cool unmelted wax at the outer edge **Figure 2b**.
c) Outside edge wax dripping: where a candle is positioned in an air draft that produces a flicking flame that causes the candle rim to melt unevenly and the melted wax to spillover **Figure 2a**.
d) Wick drowning: small or short wicks being overcome and extinguished by melt-wax thereby causing the remainder of the candle to become waste wax **Figure 2c**.
e) Candles must not be left unattended during combustion due to the inherent fire risk.

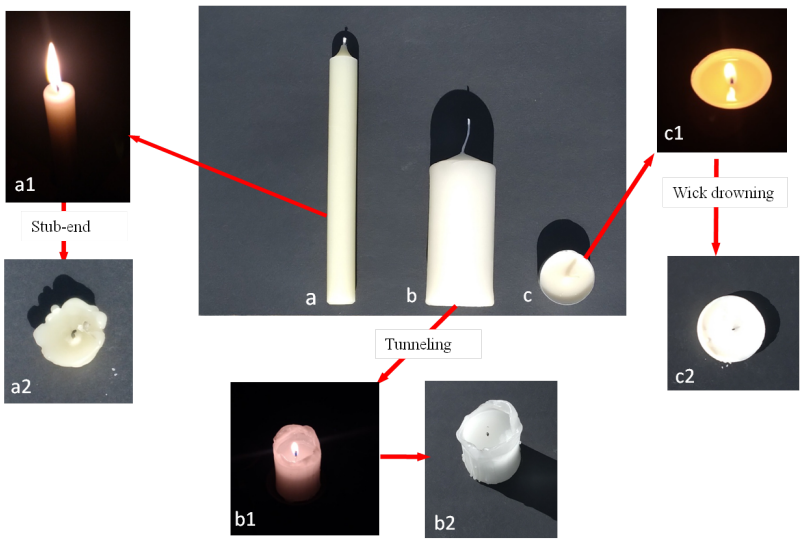

Figure 2. **(a)** Montage of wax candle types, and burning errors that lead to wax waste; **(b)** Free-standing church candle stub-end free-standing pillar candle tunneling; **(c)** Tealight wick drowning.

4. Solar recovery of mixed-wax fragments

This section describes the solar recovery of mixed-wax (paraffin, palm, and soy wax) candle fragments (100 g and 150 g) which were placed in a separate 60 g aluminum foil container. The fragments are solar-melted on 1st to 15th March 2025, and a further batch on the 18th December 2025. Two stainless-steel analogue-dial temperature probes were used to measure the absorber plate and wax temperature. The probes have a temperature range of 0 to 120 °C and 0 to 100 °C, each with an accuracy of 1 °C. The SBC-m was preheated from 8.00 a.m. to reach the target absorber plate temperature of 85–89 °C by positioning the SBC-m front face towards the Sun with the external reflector panel set to a zenith angle (φ_z) of 0 degrees to create an A_i value of 0.196 m^2. As the aim is to reach an SBC internal temperature < 100 °C, the SBC-m is aligned to the Sun's azimuth position every half-hour. Once the SBC-m is preheated, the double-glazed window is opened and the aluminum foil container with its mixed-wax fragments is placed on the preheated absorber plate. Then the window was refitted at t = 10.25 a.m. and the solar irradiance values were obtained by consulting SunCalc open-source software (https://www.suncalc.org). During the solar recovery process a number of 10 cm long and 2 mm diameter kitchen cotton wicks are added to the wax fragments which become soaked with the liquefied wax, and subsequently used as new wicks in the wax re-casting process.

Figure 3 depicts the SBC-m temperature profiles of the wax fragment melting process. From this series of measurements a number of thermal features within the solar heating process are time-stamped. Firstly, the ambient temperature (green filled squares and circles) increases by a few Celsius rough out the solar heating process. Secondly, as the containers are placed in the SBC, the absorber plate temperature (red filled squares and circles) falls due to heat escaping to the outside environment, typically 94 to 82 °C, and 89 to 75 °C. Upon refitting the double-glazed window the internal SBC temperature increases from ambient to 92 °C and 93 °C at t = 11.75 a.m., respectively. In the initial 30-min of mixed-wax heating (black filled squares and circles), $\Delta T/\delta t$ values of 0.025

and 0.031 are obtained respectively and the solid wax fragments become less hard, more compressible, and partially liquefied. Above 68–70 °C, the $\Delta T/\delta t$ rate dramatically falls to 0.0018 and 0.0021 and wax melt changes to a translucent liquid, or dark ivory depending on melt impurities.

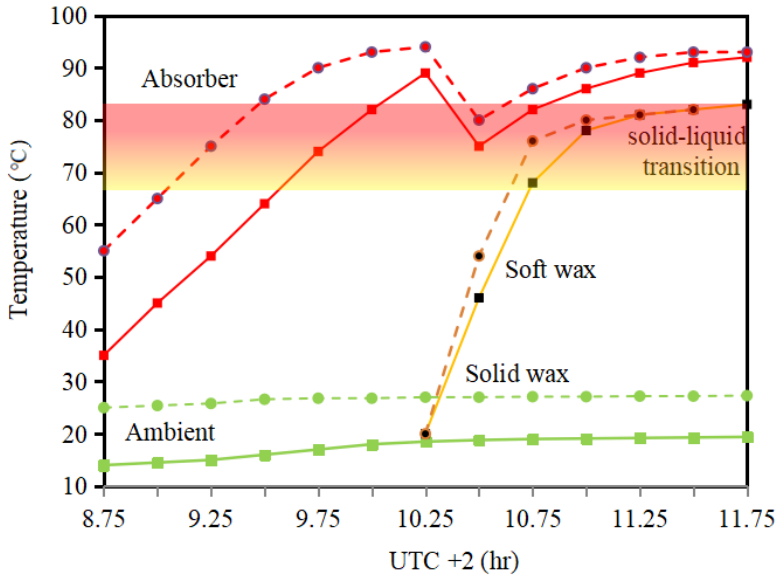

Figure 3. SBC temperature profiles obtained during the mixed-wax candle fragment melting process.

Note: Absorber plate temperature = red filled squares and circles, wax temperature = black filled squares and circles, and ambient temperature = green filled squares and circles. Solid-line = 1.3.2025 (924 W·m^{-2}), dashed-line = 15.3.2025 (950 W·m^{-2}). The graded region indicates the wax solid-liquid transition.

Figure 4 illustrates the solar mixed-wax melting process at room temperature (RT), 40 °C, 78 °C, and 82 °C. With the mixed-wax fragments liquefied, the soaked wicks and other debris sink to the bottom of the container, from where the soaked wicks are pulled using tweezers, straightened, and put to one side for the candle re-casting process.

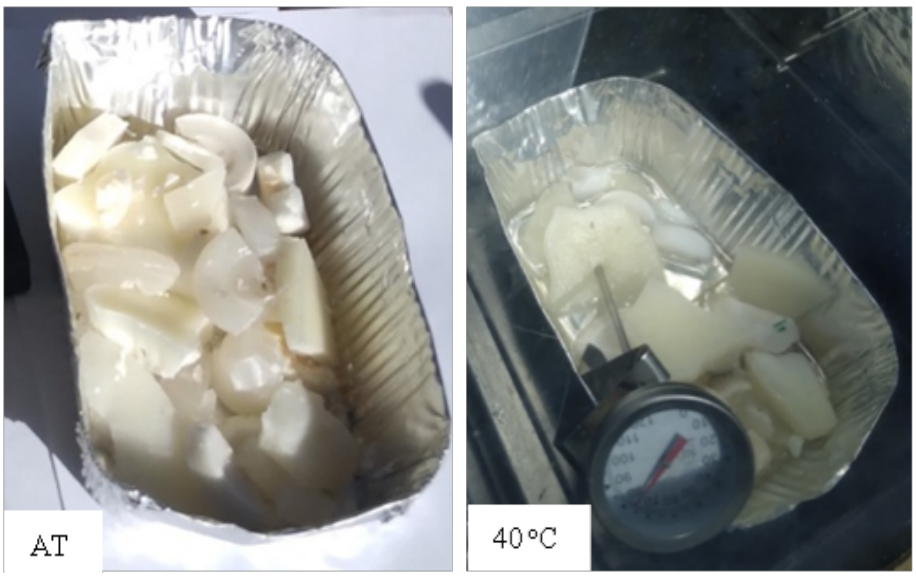

(a) **(b)**

Figure 4. *Cont.*

(c) **(d)**

Figure 4. Four photographs of the mixed-wax solar-melting process. **(a)** Mixed-wax appearance at ambient temperature (AT); **(b)** Wax appearance at 40 °C; **(c)** Wax appearance at 78 °C; **(d)** Wax appearance at 82 °C.

4.1. Estimation of candle wax melting power, energy budget, and energy density

This section uses the thermodynamic data in **Table 1** to estimate the heat required to melt the mixed-wax candle fragments in terms of required power, process energy budget, and energy density. To achieve this goal two mathematical approaches are used.

The first approach uses sensible heat calculations based on the calorimetric open-water dish load method [1,2], as shown in Equation (4).

$$P = mC\,\frac{\Delta T}{\delta t} \tag{4}$$

Where P is the applied power measured in W, or J.s^{-1}, m is the mass (g) of material, C is the heat capacity of the material being heated, ΔT is the change in heated material (final temperature minus the initial temperature), and δt is the heating time interval (s). Where temperature varies with time in a dynamic reaction, it is normal to take the tangent of the initial temperature curve (t = 10.25 a.m.) to obtain P. Using this method, P is measured in Watts (J.s^{-1}) multiplied by process time measured in seconds to yield the process energy budget measured in Joules (J). Dividing this value by the mass of material being heated, the process energy density, measured in kJ.g^{-1} is obtained for paraffin and a mixed-wax blend **Table 2**. Here it can be seen that the normalized energy density column reveals that paraffin calculations produce the lowest value for the two days of solar wax melting (0.337 and 0.35 kJ.g^{-1}) as compared to the palm and soy wax calculations (0.432 and 0.448 kJ.g^{-1}). The difference can be directly attributed to the difference in the Specific Heat Capacity of the two wax formulations **Table 2,** column 5. The average values for the two wax formulations over the two days are 0.3435 ± 0.11 and 0.44 ± 0.11 kJ.g^{-1}. It is important to note, that this sequence of calculations

provides no information on the melting process itself.

Table 2. Sensible heat estimation of required power, energy budget, and energy density based on sensible temperature method: specific heat capacity of paraffin wax and averaged mixed-wax formulation.

Day	Mass (g)	Initial $\Delta T/\delta t$	Total time (s)	Heat capacity ($J.g^{-1}.°C^{-1}$)	Power ($J.s^{-1}$)	Energy (kJ)	Energy density ($kJ.g^{-1}$)
1.3.2025 913 $W·m^{-2}$	100	0.025	5,400	2.5*	6.25	33.75	0.337
1.3.2025 913 $W·m^{-2}$	100	0.025	5,400	3.2**	8.0	43.2	0.432
15.3.2025 940 $W·m^{-2}$	150	0.031	4,500	2.5*	11.66	52.5	0.350
15.3.2025 940 $W·m^{-2}$	150	0.031	4,500	3.2**	14.9	67.2	0.448

Note: Paraffin wax*. Plus paraffin wax, palm wax and soy wax (Mixed-wax formulation)**.

The second method uses a two-stage mathematical approach. The first stage is to extrapolate the initial curve to the mixed-wax melting temperature of 82 °C to calculate applied power in Watts ($J.s^{-1}$) then multiplying this number by δt' (2,700 s (45 min)) to obtain the melting energy during this heating period (**Table 3,** column 5). The second stage is to use the latent heat of fusion of the mixed-wax mass to calculate the melting energy (**Table 3**, column 6). The total energy is summed (**Table 3**, column 7), followed by normalizing the energy values to the paraffin and mixed-wax mass (**Table 3**, column 8).

Table 3. Second estimation of energy budget, and energy density based on specific heat capacity and latent heat of fusion.

Day	Mass (g)	Initial $\Delta T/\delta t$	δt' (s)	Initial energy (kJ)	Melting energy (kJ)	Total energy (kJ)	Energy density ($kJ.g^{-1}$)
1.3.2025 913 $W·m^{-2}$	100	0.025	2,700	24*–30**	15.6*–18.5**	39.6*–48.5**	0.396*–0.485**
15.3.2025 940 $W·m^{-2}$	150	0.031	2,700	35*–44.8**	23.4*–27.5**	58.4*–68.3	0.389*–0.455**

Note. δt'= 45 min (2,700 s) to reach 82 °C. Paraffin wax*. Mixed-wax formulation**.

These two methods of calculating the total energy and energy density (**Tables 2** and **3)** yield an estimated energy density range of 0.389–0.396 $kJ.g^{-1}$ for paraffin, and 0.455–0.485 $kJ.g^{-1}$ for mixed-wax blends. These results underpin both the experimental procedure and mathematical analysis and instill a high degree of confidence in the outcome.

5. Wax recovery and re-casting on the 18th December 2025

The island of Crete is known for its winter storm systems from December through March [2]. During the early days of December 2025 Greece experienced the storm system 'Byron' which brought snow to the Lefka Ori mountain range (2,453 m), and Mt. Psiloritis (2,456 m), along with persistent cloud cover throughout the mountain range. In this section, two sequential 250 g batch mixed-wax recovery and its reuse are described for the 18th of December 2025; this date being 2–3 days before the 2025

winter solstice.

5.1. Batch solar melting of mixed wax fragments

Figure 5 depicts the temperature profile for the sequential solar batch of mixed-wax recovery. Solar preheating of the SBC-m started at t = 7.45 a.m. and finished at t = 10.15 a.m. The solar irradiance reference at the first mixed-wax insertion (t = 10.15 a.m.) = 820 W·m^{-2}, and second mixed-wax insertion (t = 12.45 a.m.) = 897 W·m^{-2}, respectively. The first batch required 120 min (7,200 s) to melt, and the second batch required 105 min (6,300 s) to melt.

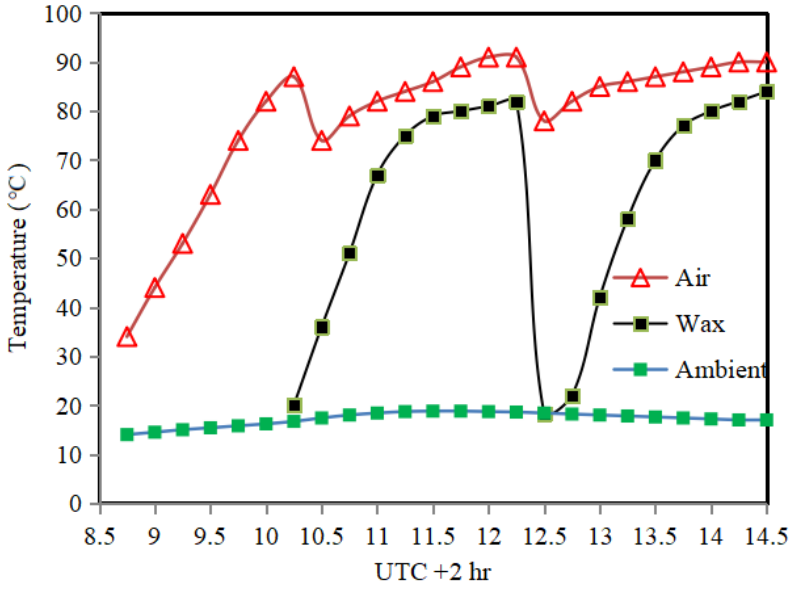

Figure 5. SBC temperature profiles for the 18.1.2025 sequential 250 g mixed-wax recovery.
Note: Absorber plate temperature = red-line with open red triangles, wax temperature = black-line with black filled squares, and ambient temperature = green-line with filled squares. Start of first batch = 823 W·m^{-2}, second batch = 897 W·m^{-2}.

Table 4 gives the full sensible heat measurements and Equation (2), along with the established average specific heat capacity of 3.2 J.g^{-1}.°C^{-1}, of mixed-wax is used to calculate the power energy budget and energy density of each 250 g of mixed-wax.

Table 4. Estimation of applied power to the mixed-wax, energy budget, and energy density based on the sensible temperature method.

Day	Mass (g)	Initial ΔT/δt	Total time (s)	Specific heat capacity (J.g^{-1}.°C^{-1})	Applied power (J.s^{-1})	Energy (kJ)	Energy density (kJ.g^{-1})
18.12.2025 823 W·m^{-2}	250	0.0172	7,200	3.2**	13.77	99.2	0.396
18.12.2025 897 W·m^{-2}	250	0.0173	6,300	3.2**	14.22	89.6	0.359
Average	250	0.01725	6,750	3.2**	13.995	94.4	0.3775

Note: Specific heat capacity for mixed-wax formulation**.

5.2. Solar power efficiency in melting mixed-wax fragments

There are a number of useful ways of comparing unloaded (empty) SBC solar performance with another unloaded SBC, the most common being the first figure of merit [42, 43]. The advantage of using this figure of merit is its ease of use and measurement; however, it is only a snapshot of the heating process and does not capture

the differences and nuances between SBC designs and local environmental factors. The estimation of the food cooking power efficiency (FCPE), is also an important parameter for comparing different loaded SBC-m [1,2]. Excluding internal SBC shadow effects, this is achieved by multiplying the local time-stamped solar irradiance (SI_t) obtained by consulting the SunCalc open-source software, by the corresponding SBC-m virtual aperture area (A_i) to obtain the SBC-m input power. This value is then divided by the applied power to the target food that is being heated (P_f). This value is then multiplied by 100 and the product is expressed as a percentage. To encompass the solar recovery of mixed-wax FCPE may be redefined as solar power efficiency (SPE) Equation (5) where P_f becomes the applied power to the target object being heated (P_{to}), in this instant the melted mixed-wax.

$$SPE \approx \left(\frac{P_{to}}{(SI_t A_i)} \right) \times 100 \tag{5}$$

Table 5 shows the calculations for the mixed-wax recovery on the 1st and 15th of March 2025, and 18th of December 2025. The data shows for 100 g of mixed-wax the SPE is 4.47% and increases to 8% for 150 g which forms an 8–8.5% cluster with the 250 g data. This SPE percentage profile mirrors the applied power to the mixed-wax indicating a volume loading effect is in operation rather than a simple direct solar irradiance proportionality response. This can be interpreted by considering that the mixed-wax recovery within the container begins as the wax fragments turn into wax islands surrounded by liquefied wax that ultimately turns into a liquid slab at the bottom of the container **Figure 4**. The observed loading effect therefore may be due to, but not limited to, two possible causes. The first arises from experimental error due to insufficient wax mass within the aluminum foil container to allow a reliable temperature measurement to be recorded [36]. The second relates to the way the wax fragment mass initial absorb the solar thermal energy and delays the transfer of thermal energy to the solid aluminum foil container. In this second scenario, the recovery process begins when the wax fragments in the container turn into wax islands surrounded by liquefied wax that ultimately turns into a liquid slab at the bottom of the container. During this time evolving process solar thermal energy is preferentially absorbed by the wax, and as the mixed-wax forms a liquefied slab more thermal energy is transferred to the bottom of the aluminum foil container. Thus, the heat transfer from the solar irradiance to the phase-changing wax and the solid aluminum foil container becomes further complex as the wax changes from fragments to a liquid slab.

Table 5. SBC-m SPE for 100, 150, and 250 g mixed-wax recovery.

Day wax mass	Solar irradiance ($W \cdot m^{-2}$)	A_i (m)	Applied power to mixed-wax (W)	SPE (%)
1.3.2025 100 g	913	0.196	8.0	4.470
15.3.2025 150 g	940	0.196	14.90	8.087
18.12.2025 250 g	823	0.196	13.77	8.536
18.12.2025 250 g	897	0.196	14.22	8.088

5.3. Liquid wax re-casting

For domestic-scale candle making (typically, two batches of 250 g per day), sourcing sufficient similar-sized and shaped permanent glass mold containers can be the rate-limiting factor in the number of candles made per day. Consequently, the use polycarbonate and silicone temporary molds extends the supply of useful containers. Here, the term 'permanent' relates to molds that are used in the re-casting of wax and their continued use in the candle burning process, and 'temporary' relates to molds that are used in the re-casting process. Polyvinylchloride containers are rejected due to their low deformation temperature (typically, 100 °C). With these provisos, silicone, polycarbonate, and glass jars are collected over-time with scratched or cracked containers rejected and recycled. When the origin and material of the container are uncertain, or there is a question as to whether the glass has undergone heat-tempering (or heat-strengthening), these containers are rejected and recycled. Once the containers have been accepted for reuse, they are cleaned and inspected for any damage again. The outcome of the sorting and cleaning process is usually a limited supply of suitable pre-used containers for the prospective candle-maker.

Generally, a wax casting process requires a wax-soaked wick suspended vertically within the candle mold from a pre-brought wick holder, and then the liquefied wax is poured. In this work, the wick holders are fabricated from surplus household material and built into the side of SBC-m to enable batch wax pouring into molds. Two types of wick holders are exemplified here, where the material used depends on locally available materials **Figure 6a**.

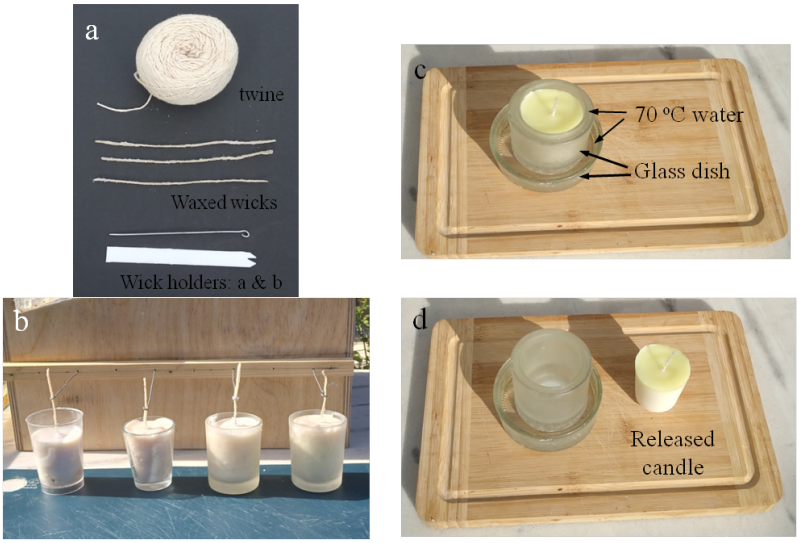

Figure 6. Photographs of wax re-casting and candle release process. **(a)** Kitchen cotton twine ball, waxed twine, and wick holders; **(b)** Poured mixed-wax into polycarbonate and glass molds of different shapes; **(c)** Post wax pouring. A 50 g blended wax candle within its glass mold is placed in 70–75 °C dual-water bath; **(d)** Blended-wax candle removed from its glass mold after approximately 45 s of treatment in the dual-water bath.

a) Repurposed food packaging strip (10 mm wide × 1 mm with V-notch at the end) to hold the wick in position.

b) Metal wire (1 mm diameter) with a ring aperture to hold the wick in position. Once the wax is poured, cooled, and hardened, the wick is cut from the ring aperture.

c) To prevent voids from forming around the wick, the molds need to be warmed to approximately 30 °C, negating a second casting of liquid wax. Once the pouring is completed, **Figure 6b**, the blended wax is allowed to cool and harden for 2 h before releasing the candle from its mold and the wick is trimmed.

5.4. Candle mold release

The release of the blended wax from glass 40–60 g wax temporary molds is performed using a dual-water bath, where the water is pre-heated to a maximum of 70 °C within the SBC-m. (N.B. for silicon polycarbonate molds, the process is unnecessary as the molds can be simply bent away from the wax candle). For the glass molds, the dual-water bath comprises an outer 90 mm diameter × 35 mm high glass vessel filled with 70 g of non-displaced hot water which acts as a thermal heat reservoir. This was used in conjunction with a second inner glass vessel, 63 mm diameter, and 67 mm high, filled with 35–48 g of hot water. The latter provides a uniform thermal heat transfer to the mold outer surface, through which heat is transferred to the container-wax interface (**Figure 6c**). After approximately 45 s of thermal heating, the blended-wax interface surface softens and liquefies enabling the candle to be pulled away from the mold, using its wick (**Figure 6d**). An important feature of this process step is the use of renewable and free energy.

6. Power and energy comparison with solar cooking of food

Section 5 of this work explored the SPE and solar energy transfer to mixed-wax fragments with the SBC-m. It is useful to place the outcomes of these calculations into context with previously reported SBC-s and SBC-w designs. In this instance cooking of the following targeted food: whole liquid eggs, white medium-grain rice, and pre-soaked brown lentils [1, 2]. **Table 6** presents the reported foodstuffs on the day of solar processing within the SBC-type plus and the associated solar cooking data: input power (SI multiplied by A_i), SPE, energy, and energy density supplied to the target and the target energy. Given the various target foods and cooking vessels used, solar cooking of eggs is dealt with separately (Section 6.1) from the solar cooking of rice and lentils (Section 6.2).

6.1. A comparison with solar-cooked whole liquid eggs without water

Table 6, row 2, and rows 5–9, tabulate the solar cooking of whole liquid eggs without water to a hard-boiled consistency data. The data reveals the applied power to eggs ranges between 9.1 and 13.7 W, where the greatest value of 13.7 W is applied in the summer month of July 2024. The SBC-w applied power lower (171–183 W) is due to the lower solar irradiance in the winter months (November and December 2025 through January 2025). When the solar cooking of whole liquid eggs is normalized to the input power and egg mass, the computed values become clustered (SPE = 6.13–6.77% and energy density = 0.46–0.55 $kJ.g^{-1}$). With this knowledge a meaningful comparison with the mixed-wax solar recovery SPE data presented in **Table 5** is possible. In this case, the mixed-wax, SPE = 4.47% for 100 g of eggs and 8–8.5% for 150–250 g of eggs, both of which bracket the solar cooking of eggs data. Given the specific heat capacity of

the mixed-wax (3.23 $J.g^{-1}.°C^{-1}$) and whole liquid eggs (3.2 $J.g^{-1}.°C^{-1}$ [44]) and their respective mass are of the same order, the normalization process appears to point to the different ways the two target product are in contact with the heated absorber plate within the SBC designs (the mixed-wax in good thermal contact through the aluminum foil container while the eggs are in poor thermal contact through eggs boxes that are used to support the eggs and prevent the egg shells from burning.

Table 6. Power and energy utilization based on using SunCalc solar irradiance values and A_i data for SBC-s and SBC-w.

SBC-x day	Food, mass and cooking vessel	Input power (SI* A_i) (W)	Applied power (W)	SPE (%)	Energy (kJ)	Energy density ($kJ.g^{-1}$)
SBC-s 27.7.2024	3 eggs 162 g egg box	199$	13.07	6.56	94.1	0.580
SBC-s 29.7.2024	White medium-grain rice 100 + 200 g water glass vessel	199$	32.07	16.11	115.48	0.385
SBC-s 7.8.2024	Pre-soaked brown lentils 100 + 300 g water glass vessel	193$	33.47	17.34	210.80	0.527
SBC-w 5.11.2024 935 $W·m^{-2}$	3 eggs 175 g egg box	183$$	11.229	6.13	90.95	0.519
SBC-w 4.12.2024 879 $W·m^{-2}$	3 eggs 160 g egg box	172$$	11.23	6.52	90.95	0.558
SBC-w 18.12.2024 873 $W·m^{-2}$	3 eggs 178 g egg box	171$$	9.14	6.69	82.22	0.462
SBC-w 6.1.2025 880 $W·m^{-2}$	3 eggs 195 g egg box	172$$	11.44	6.65	92.66	0.475
SBC-w 11.1.2025 885 $W·m^{-2}$	3 eggs 188 g egg box	173$$	11.72	6.77	94.92	0.505

Note: $ A_i = 0.192 m^2. $$ A_i = 0.196 m^2.

6.2. Comparison with solar-cooked white medium-grain rice and brown lentils

The brown rice and pre-soaked lentils are cooked using the water absorption method (where only sufficient water is used to cook, leaving no excess water to be drained as shown in **Table 6**, rows 3 and 4 for the summer month of July 2024. In the case of 100 g of white medium-grain rice 200 g of water is used, whereas for 100 g of brown lentils 300 g of water is used. The thermodynamic data reveal a comparative increase in applied power and SPE is compared to the summer solar-cooked eggs. Here it is reasonable to assume this is part due to the presence of water at a higher temperature that has a specific heat capacity of 4.184 $J.g^{-1}.°C^{-1}$ [1,2]. For these foods it is noted there is a difference in their required energy and resulting energy densities, both of which are connected to their extended solar cooking times.

7. Conclusion

This paper describes the novel use of a low-cost off-grid solar box for the solar recovery of mixed wax (paraffin, soy and palm wax) and their re-casting into new candles within a repurposed SBC. The novelty arises from no external photovoltaic panels or fresnel reflector are used in the melting or recovery of the wax. Thus the cost of SBC ownership is kept to a minimum along with minimizing the environmental foot-print of the SBC. Incorporated within this work are four specific aims (objectives).

First to undertake solar experiments on the Mediterranean island of Crete (35.31° N, 24.31° E, altitude 150 m) in the astronomical winter season of 2025. The wax recovery and re-casting is undertaken on sunny days with typical 820–940 $W \cdot m^{-2}$ solar irradiance. In addition, a circular economy of candle molds reused and eventual recycle is possible, whereas the kitchen twine is a single-use component of the candle-making process.

The second aim was to estimate the SBC required power, process energy budget, and energy density for the recovery of mixed-wax fragments, using both sensible heat and phase-change calculations. Here both sensible heat and phase-change thermodynamic analyses of >150 g mixed-wax fragments, provide a zero-dimensional (0D)-model of the energy imparted into the mixed-wax which is of the order of 0.35–0.44 $kJ.g^{-1}$. For 100 g of mixed-wax fragments, loading effects are observed, which the 0D-model does not capture, implying additional spatial information is required, nevertheless, the thermodynamic analyses of the solar wax-recovery provide initial screening calculations that point to further fully characterize SBC melting of mixed-wax.

The third aim is to undertake blended wax re-casting studies; under the conditions established in the first and second aims. Two batches of 250 g of mixed-wax can be liquefied in the morning followed by conversion into eight new candles with a total weight of 490 g, equating to 98% mixed-wax reuse.

In the case of the fourth aim, a comparison with reported solar cooking of whole liquid eggs without water, and white medium-grain rice and brown lentil using the water absorption method within SBC-s, and SBC-w designs has been made. For whole liquid eggs the comparison reveals similar SPE and energy density values are obtained. However, in the case of rice and lentils the additional water mass increases the applied power and SPE values; in addition the solar cooking time impacts the required energy and energy density.

Bringing together the outcomes of SBC-m experiments and analysis there are two noteworthy observations. Firstly, the experimental design produces a power and energy metric that enables researcher in the field solar box cooker processing of organic material to compare and contrast different SBC experiment; secondly on a practical level, repurposing a SBC from simple food cooking and culinary leaf dehydration into the circular economy of unconsumed mixed-wax fragment recovery and reuse extends the SBC function, although a dedicated heat absorber plate, and wax melt foil container are required to prevent contamination of foodstuff.

Future work is envisaged in the following areas: firstly study the solar recovery

of blended food-grade paraffin and microcrystalline-wax commonly used to provide a protective barrier on cheese products. Second, scaling-out, rather than scaling-up, to 1 kg of mixed-wax using the summer solstice period where solar irradiance and longer daylight hrs are maximized. Thirdly, utilize building information modelling (BIM) software to identify and capture SBC-m internal shadows and relate this spatial information to the mixed-wax loading observations.

Author contributions: VJL, JFL, and DPD conceived and planned the solar experiments. JM contributed to the environmental approach taken thoughout the solar experiments. VJL wrote the manuscript with input from all authors. All authors have read and agreed to the published version of the manuscript.

Funding: This work received no external funding.

Institutional review board statement: Not applicable.

Informed consent statement: Not applicable.

Data availability statement: The data used in this study are available from the corresponding author upon reasonable request.

Conflict of interest: The authors declare they have no conflict of interest.

References

1. Law VJ, Lalor JF, Dowling DP. Inclined window solar box cooker with one external reflector designed for the Mediterranean latitudes. Journal of Power and Energy Engineering. 2024; 11(12): 1–33.
2. Lalor JF, Law VJ, Dowling DP. Winterizing and use of a solar box cooker on the island of Crete, Greece. American Journal of Analytical Chemistry. 2025; 16(3): 23–41.
3. Ouafi N, Benaouda N, Moghrani H, et al. Experimental analysis of solar drying kinetic of Algerian bay leaves (*Laurus nobilis* L.). Journal of Renewable Energies. 2016; 19(2): 251–264.
4. Law VJ, Lalor JF, Dowling DP. Solar box cooker dehydration of culinary leaves: Leaf morphometrics and relative humidity endpoint detection. In: Proceedings of the 6th Edition of Chemistry World Conference; 18–20 June 2026; Barcelona, Spain.
5. Kumar A, Saxena A, Pandey SD, et al. Design and performance characteristics of a solar box cooker with phase change material: A feasibility study for Uttarakhand region, India. Applied Thermal Engineering. 2022; 208: 118196.
6. Misra N, Anand A, Pandey S, et al. Box-type solar cookers: An overview of technological advancement, energy, environmental, and economic benefits. Energies. 2023; 16(4): 1697.
7. Al-Rajhi MAI, El-Serey SM, Elsheikha AM. Application of solar energy to liquefy beewax. Turkish Journal of Agricultural Engineering Research. 2023; 4(2): 203–224.
8. Al-Rajhi MAI, El-Serey SM, Elsheikha AM. Solar beeswax melter. Agricultural Engineering International: CIGR Journal. 2024; 26(3): 107–122.
9. Khan KA, Hazrat Ali M, Obaydullah AKM, et al. Candle production using solar thermal systems. In: Proceedings of the 1st International Conference on Energy Systems, Drives and Automations ESDA2018; 29–30 December 2018; Kolkata, India. pp. 55–66.
10. Arabacigil B, Yuksel N, Avci A. The use of paraffin wax in a new solar cooker with inner and outer reflectors. Thermal Science. 2025; 19(5): 1663–1671.
11. Cuce PM, Kolayli S, Cuce E. Enhanced performance figures of solar cookers through latent heat storage and low-cost booster reflectors. International Journal of Low-Carbon Technologies. 2022; 15(3): 427–433.
12. Soro D, Sidibé M, Doumbia Y, et al. Theoretical and experimental studies of a box-type solar cooker in unfavorable climatic conditions. Smart Grid and Renewable Energy. 2020; 11: 51–60.
13. Chatelain T, Mauree D, Taylor S, et al. Solar cooking potential in Switzerland: Nodal modelling and optimization.

Solar Energy. 2019; 194: 788–803.
14. Lagouvardos K, Dafis S, Giannaros C, et al. Investigating the role of extreme synoptic patterns and complex topography during two heavy rainfall events in Crete in February 2019. Climate. 2020; 8(7): 87.
15. Hassanain AA. Drying sage (*Salvia officinalis* L.) in passive solar dryers. Research in Agricultural Engineering. 2011; 57(1): 19–29.
16. Castillo-Téllez M, Martínez OS, Miranda-Mandujano E, et al. Solar drying of oregano leaves (*Plectranthus amboinicus*, Lour): Analysis of experimental performance under a tropical climate. Energy Exploration and Exploitation. 2024; 42(5): 1895–1921.
17. Nastos PT, Kampanis NA, Giaouzaki KN, et al. Environmental impacts on human health during a Saharan dust episode at Crete Island, Greece. Meteorologische Zeitschrift. 2011; 20(5): 517–529.
18. Chatoutsidou SE, Saridaki A, Raisi L, et al. Variations, seasonal shifts and ambient conditions affecting airborne microorganisms and particles at a southeastern Mediterranean site. Science of the Total Environment. 2013; 892(2): 164797.
19. Marsh R. Sculpting sand candles. Design. 1976; 76(2): 19–21. doi: 10.1080/00119253.1974.10118733
20. Vourdoubas J. The degrowth of tourism industry in the island of Crete, Greece: Is it desirable and feasible? International Journal of Current Science Research and Review. 2025; 8(2): 749–758.
21. Abdussalam-Mohammed W, Alia AQ, Errayes AO. Green chemistry: Principles, applications, and disadvantages. Chemical Methodologies. 2020; 4(4): 408–423.
22. Sheldon RA. The E factor at 30: A passion for pollution prevention. Green Chemistry. 2023; 25(5): 1704–1728.
23. Hallikainen H, Ovaska M, Laukkanen M. What motivates second hand gift giving? European Journal of Marketing. 2025; 59(13): 488–513.
24. Bejenari V, Rusu D, Anghel I, et al. Fire-starting briquettes with high spent coffee-ground content and various wax types. Biofuels, Bioproducts and Biorefining. 2025; 19(6): 2076–2091.
25. Benbaha A, Yettou F, Azoui B, et al. Novel mixed solar cooker: Experimental, energy, exergy, and economic analysis. Heat Transfer. 2023; 53(4): 2095–2127.
26. Kumar A, Saxena A, Pandey SD, et al. Cooking performance assessment of a phase change material integrated hot box cooker. Environmental Science and Pollution Research. 2024; 31: 62392–62407.
27. Andersen Y, Omelekhina Y, Rasmussen BB, et al. Emissions of soot, PAHs, ultrafine particles, NOx, and other health relevant compounds from stressed burning of candles in indoor air. Indoor Air. 2021; 31(6): 2033–2048.
28. Eremkin A, Ponomareva I. Theoretical and experimental substantiation of the system of local removal of harmful substances during the combustion of candles in the worship hall of Orthodox churches and cathedrals. E3S Web of Conferences. 2021; 263: 04013.
29. Wattanakasiwich P, Kongkhumbod P, Pussadee N. Heating up a lantern with a tealight candle. Revista Mexicana de Física E. 2022; 19(6): 010206.
30. Meijaard E, Sheil D. The moral minefield of ethical oil palm and sustainable development. Frontiers in Forests and Global Change. 2019; 2: 22.
31. Brown JF, Paxton RJ. The conservation of bees: A global perspective. Apidologie. 2009; 40: 410–416.
32. Zmywaczyk J, Zbińkowski P, Smogór H. Cooling of high-power LED lamp using a commercial paraffin wax. International Journal of Thermophysics. 2017; 38(3): 45.
33. Eštoková A, Kapalo P. Investigation of the thermal properties of candle wax material. IOP Conference Series: Materials Science and Engineering. 2022; 1252: 012013.
34. Rezaei K, Wang T, Johnson LA. Hydrogenated vegetable oils as candle wax. Journal of the American Oil Chemists' Society. 2002; 79(12): 1241–1247.
35. Birk JP, Lawson AE. The persistence of the candle-and-cylinder misconception. Journal of Chemical Education. 1999; 76(7): 914–916.
36. Law VJ, Dowling DP. Application of microwave oven plasma reactors for the formation of carbon-based nanomaterials. In: Proceedings of the 13th Chaotic Modeling and Simulation International Conference. Springer International Publishing; 2021. pp. 467–486.
37. Trisnadewi T, Kusrini E, Nurjaya DM, et al. Comparison of phase change materials of modified soy wax using graphene and maxene for thermal energy storage materials in buildings. International Journal of Technology. 2023; 14(3): 596–605.
38. Sena B, Dhal S, Sahu D, et al. Variations in microstructural and physicochemical properties of soy wax/soybean oil-derived oleogels using soy lecithin. Polymers. 2022; 14(19): 3928.

39. Alakali JS, Eze SO, Ngadi MO. Influence of variety and processing methods on specific heat capacity of crude palm oil. International Journal of Chemical Engineering and Applications. 2012; 3(5): 300–302.
40. Abdullah D, Marwazi M, Deny F, et al. The effects of aromatherapy candles as a complementary therapy for sleep disturbances: A literature review. Nusantara Hasana Journal. 2024; 4(2): 159–169.
41. Putra N, Sandi AF, Ariantara B, et al. Performance of beeswax phase change material (PCM) and heat pipe as passive battery cooling system for electric vehicle. Case Studies in Thermal Engineering. 2020; 21: 100655.
42. Folaranmi J. Performance evaluation of a double-glazed box-type solar oven with reflector. Journal of Renewable Energy. 2013; 2013(1): 184352.
43. Collares-Pereira M, Cavaco A, Tavares A. Figures of merit and their relevance in the context of a standard testing and performance comparison methods for solar box-cookers. Solar Energy. 2018; 166: 21–27.
44. Coimbra JSR, Gabas AL, Minim LA, et al. Density, heat capacity and thermal conductivity of liquid egg products. Journal of Food Engineering. 2006; 74: 186–190.